

COVER PAGE

Document downloaded by @DAEL

Sat Nov 28 11:04:20 2026
For personal use

When automatic English translation is provided, only the original document is authentic.
The EAA cannot be held responsible of any translation error

Bibliographical reference

Experimental Validation of an Acoustical Micro-Macro Model for Random Hollow Fibre Structures, Simon Campeau, Raymond Panneton and Saïd Elkoun, Acta Acustica **vol. 105** (Number 1), 2019, pp. 240-247

DOI
https://doi.org/10.3813/AAA.919305

Acta Acustica united with Acustica
Vol. 105 (2019) 240 – 247

DOI 10.3813/AAA.919305

Experimental Validation of an Acoustical Micro-Macro Model for Random Hollow Fibre Structures

Simon Campeau, Raymond Panneton, Saïd Elkoun
Groupe d'Acoustique de l'Université de Sherbrooke (GAUS), Department of Mechanical Engineering, Université de Sherbrooke, Québec J1K 2R1, Canada. Simon.Campeau@USherbrooke.ca

Summary
This work investigates the validity of recent micro-macro solid fibre relationships for the case of a nonwoven fibre structure made from milkweed floss, a natural hollow fibre. The hypothesis that hollowness of the fibre has only small effects on the acoustics of the material is verified. This is done to ensure that the use of a single porosity model is justified. Therefore, the micro-macro solid fibre relationships are used to retrieve the macroscopic transport and acoustic properties of the fibrous material by the only knowledge of four measured microstructural features: porosity, effective inner and outer radii of the hollow fibre, and fibre orientation. Sound absorption coefficient predicted by two rigid-frame porous models are compared with standing wave tube measurements. The two rigid-frame porous models are the six-parameter Johnson-Lafarge model and the one-parameter Miki model. The parameters of these models are obtained by the micro-macro solid fibre relationships. The fibres of the tested nonwoven materials are mainly arranged randomly in parallel planes (i.e., layered fibrous media showing transverse isotropy). The predictions obtained by both rigid-frame porous models agree with experimental data when the acoustic excitation is normal to the layered fibrous media as well as when excitation is perpendicular.
© 2018 The Author(s). Published by S. Hirzel Verlag · EAA. This is an open access article under the terms of the Creative Commons Attribution (CC BY 4.0) license (https://creativecommons.org/licenses/by/4.0/).

PACS no. 43.50.Gf, 43.55.Ev, 43.58.Bh

1. Introduction

In the recent effort to treat noise problems with sustainable solutions, much progress are made about recycled and natural fibres for acoustical purpose. Although there is still work to be done about their characterization, studies show that those alternatives can be competitive with rock and glass wools, being moreover light, safe for human health and already available on the market [1]. With a view to go one-step further in sustainable acoustic materials, some researchers study natural hollow fibres like kapok and estabragh, showing their acoustical potential, especially for their low density. To better understand the acoustical behavior of natural hollow fibres, Liu *et al*. [2] model kapok-based nonwovens by using a correction of the thermal conductivity of the fibre on the Biot-Allard model for cylindrical pores. The use of such a model requires the knowledge of five material parameters (static airflow resistivity, porosity, tortuosity, x, and y). To simplify their acoustical modelling of kapok-based nonwoven materials, the same authors [3] propose new coefficients for the one-parameter (static airflow resistivity) empirical model of Delany-Bazley. Their modified Delany-Bazley model correlates well with normal incidence sound absorption measurements made in impedance tube on kapok-based nonwoven materials; however, their model gives no information between the microstructure, or arrangement of the fibres, and the acoustic properties of the materials. In a recent work, Luu *et al*. [4] use a multiscale approach to develop micro-macro relationships between microstructural features (fibre radius, porosity, fibre angular orientation) and the acoustic properties of a random fibre structures. Their relationships are obtained from finite element solutions of the transport equations on representative volume elements (RVEs) of random solid fibre structures. Despite their relationships correlate well with previous published results on random solid fibre structures, no experimental validation are presented for hollow fibre structures, and the effect of the hollowness is not taken into account.

The main objective of this research is to validate experimentally the micro-macro relationships by Luu *et al*. for the case of natural hollow fibres found in North America: milkweed seed hair, also known as asclepias. One of the common assumptions about hollow fibres is that hollowness enhances noise absorption. In this paper, the hypothesis that hollowness of the fibres has minimal effects on the acoustics is first put forward, mainly because of the small dimensions of the fibre inner diameter. In this case, the fi-

Received 11 September 2017,
accepted 12 November 2018.

© 2018 The Author(s). Published by S. Hirzel Verlag · EAA.
This is an open access article under the terms of the CC BY 4.0 license.

bre external porosity is therefore used. This hypothesis is verified by acoustical measurements and by including hollowness effects to the model with a mixing rule, neglecting diffusion effects.

This paper is organized as follow. Section 1 recalls the theory of the micro-macro relationships developed by Luu *et al.*. Section 2 describes the materials and methods used in this research. Section 3 presents and discusses the results.

2. Theory

2.1. Micro-macro relationships for random solid fibre structures

Polydisperse or bi-disperse fibrous media, made from solid fibres randomly distributed, can be described by three microstructural parameters: the effective fibre radius r, the open porosity ϕ, and the statistically averaged fibre orientation coefficient Ω_{zz} [5, 6]. For transversely isotropic material, Ω_{zz} represents the statistical proportion of fibres oriented along the z-axis (here, the wave propagation axis). Depending on the orientation of the fibres, such materials range from a two-directional (2d) random structure (Ω_{zz}=0, layered fibrous media) to a unidirectional (1d) random structure (Ω_{zz}=1) through a three-dimensional (3d) random structure (Ω_{zz}=1/3). In terms of acoustic propagation, this range of structures is transversely isotropic except for the 3d case which is fully isotropic. An example of a 2d structure is shown in Figure 1. In this case, the wave propagations along directions e_x and e_y are identical.

Based on the three aformentionned microstructural parameters, micro-macro relationships were derived to estimate the six non-acoustical parameters of random solid fibre structures [4]. These parameters are the static airflow resistivity σ, the torsuosity α_∞, the viscous characteristic length Λ, the thermal characteristic length Λ', and the thermal static permeability k_0'. The micro-macro relationships to estimate these parameters are recalled here,

$$\frac{\sigma}{\eta} = \frac{2.9027^{-\Omega_{zz}^2} 1.1537^{-\Omega_{zz}}}{0.0895 r^2 \left(\frac{\phi^3}{(1-\phi)^2}\right)^{0.6295}} \quad \text{along } e_z, \tag{1}$$

$$\frac{\sigma}{\eta} = \frac{1}{0.0951 r^2 \left(\frac{\phi^3}{(1-\phi)^2}\right)^{0.6520}} \quad \text{along } e_x \text{ and } e_y, \tag{2}$$

$$k_0^{'} = \frac{r^2}{14.4718} \frac{\phi^3}{(1.0216-\phi)^2}, \tag{3}$$

$$\Lambda' = \frac{\phi r}{1.0036-\phi}, \tag{4}$$

$$\frac{\Lambda'}{\Lambda} = (1+M), \tag{5}$$

$$\alpha_\infty = \left(\frac{1}{\phi}\right)^M, \tag{6}$$

where η is the dynamic viscosity of saturating air, $M = -0.0596\Omega_{zz}^2 - 0.9994\Omega_{zz} + 1.0590$ along e_z, or $M = 0.2631\Omega_{zz}^2 + 0.2895\Omega_{zz} + 0.5957$ along e_x and e_y. Equations (1) to (6) correspond to Equations (26), (25), (31), (12), (19), and (17) of reference [4] respectively. They are written here in a more compact form and the viscous permeability is written in the form of the static airflow resistivity.

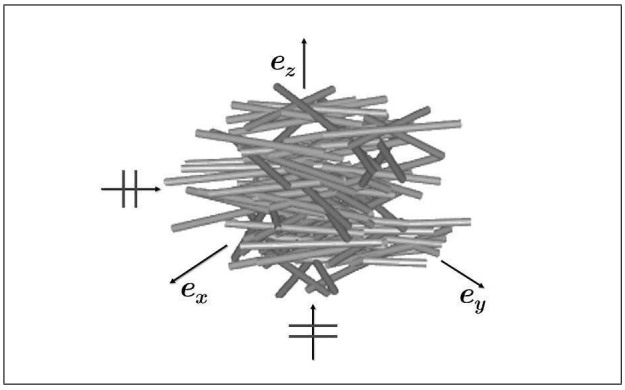

Figure 1. Example of a random fibre structure showing transverse isotropy with fibre orientation coefficient $\Omega_{zz} = 0$ (2d structure, layered fibrous media).

2.2. Equivalent fluid properties

The above non-acoustical parameters can be used to feed the so-called Johnson-Lafarge equivalent fluid model for porous media. In this context, the porous medium is characterized by the effective dynamic density and bulk modulus [7, 8] respectively given by

$$\rho_e = \rho_0 \left(\alpha_\infty + \frac{\sigma\phi}{\mathrm{j}\omega\rho_0} \sqrt{1 + \left(\frac{2\alpha_\infty \eta}{\sigma\phi\Lambda}\right)^2 \frac{\mathrm{j}\omega\rho_0}{\eta}} \right) \tag{7}$$

and

$$K_e = \frac{\gamma P_0}{\gamma - (\gamma-1)\left(1 + \frac{\phi\eta}{\mathrm{j}\omega\rho_0 k_0' B^2} \sqrt{1 + \left(\frac{2k_0'}{\phi\Lambda'}\right)^2 \frac{\mathrm{j}\omega\rho_0 B^2}{\eta}}\right)^{-1}}, \tag{8}$$

where ρ_0, γ, and B^2 are the density, specific heat ratio, and Prandtl number of saturating air, $\mathrm{j} = \sqrt{-1}$, and ω is the angular frequency of the acoustic excitation.

Since the fibres are hollow, their inner part may modify the dynamic properties of the fibre structure. In this case, the hollow fibre structure may be seen as a double porosity medium with a mesoporosity formed by the inter-fibre voids, and a microprosity formed by the intra-fibre voids. The added effect of the fibre hollowness can be taken into account using the mixing rule method (MRM) [9]. This added effect would be maximum in the case where the fibres are parallel to the acoustical excitation. In this context, following MRM, the equivalent dynamic properties of the double-porosity hollow fibre structure are given by

$$\rho_{eq} = \left(\frac{\phi_m}{\rho_{e,m}} + \frac{(1-\phi_m)\phi_\mu}{\rho_{e,\mu}} \right)^{-1} \tag{9}$$

and

$$K_{eq} = \left(\frac{\phi_m}{K_{e,m}} + \frac{(1-\phi_m)\,\phi_\mu}{K_{e,\mu}} \right)^{-1}, \tag{10}$$

where subscripts m and μ denote properties relative to the mesoporous and microporous media, ϕ_m is the mesoporosity or inter-fibre porosity, $\phi_\mu = (1 - t/r)^2$ is the microporosity, and t is the fibre wall thickness. The effective dynamic properties of the mesoporous medium are deduced from Equations (7) and (8) with the non-acoustical properties given by Equations (1)–(6), and porosity $\phi = \phi_m$. Assuming the hollow fibres are comparable to straight circular hollow cylinders, the effective dynamic properties of the microporous medium are also deduced from Equations (7) and (8) with the following non-acoustical properties: $\phi = \phi_\mu$, $\sigma = 8\eta/\phi_\mu/(r-t)^2$, $\alpha_\infty = 1$, $\Lambda = \Lambda' = r - t$, and $k'_o = \phi_\mu (r-t)^2/8$.

It is worth mentioning that if the fibres are solid (i.e., $t = r$, single porosity medium), only the first term in Equations (9) and (10) is taken into account to compute the equivalent dynamic fluid properties of the fibre structure.

2.3. Acoustic properties

From the equivalent dynamic properties, the normal incidence sound absorption coefficient can be deduced from

$$\alpha = 1 - \left| \frac{Z\cos(qh) - \mathrm{j}\sin(qh)}{Z\cos(qh) + \mathrm{j}\sin(qh)} \right|^2 \tag{11}$$

with the characteristic impedance

$$Z = \frac{1}{\rho_0 c_0} \sqrt{\rho_{eq} K_{eq}} \tag{12}$$

and the complex wavenumber

$$q = \omega \sqrt{\frac{\rho_{eq}}{K_{eq}}}. \tag{13}$$

where h is the thickness of the fibrous layer, and c_0 is the speed of sound in the air.

3. Materials and Methods

3.1. Produced fibrous materials

The fibre used in this work is milkweed (*Asclepias Syriaca*) seed hair, a natural hollow fibre. SEM images at zoom 30x and 2500x of this fibre are shown in Figure 2 (top row). Its average external radius is $r = 12.5$ μm with an average wall thickness of $t = 1.6$ μm and fibre length ranging from 2 to 4 cm [5]. The density of the solid part of the fibre is $\rho_{s1} = 1460$ kg/m^3 [10].

Two types of samples are produced for this work. The first type is used to validate the micro-macro relationships at different densities based on static airflow resistivity tests, and sound absorption tests in impedance tube. The second type is firstly used to verify if the hollowness

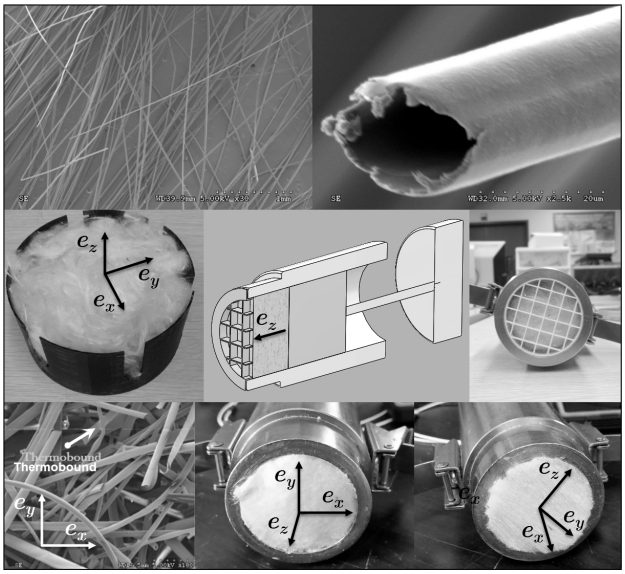

Figure 2. Top row: SEM images at zoom 30x (left) and 2500x (right) of milkweed seed hairs. Middle row: Sample of type 1 produced from compacted bulk milkweed fibres. Bottom row: Sample of type 2 (nonwoven) produced from milkweed fibres and thermobonding bicomponent fibres. The corresponding SEM image is at zoom 180x.

of the fibres affects the acoustic propagation. Secondly, it is used to validate the micro-macro relationships in the normal and transverse directions. The first validation is based on the measurement of the total open porosity and kinematic porosity using an ultrasound technique. Here, the kinematic porosity is the part of the total open porosity where fluid can circulate. A detailed description of these two porosities is given elsewhere [11]. The second validation is based on sound absorption measurements in normal and transverse directions in impedance tube. The measurement methods are discussed below.

The first type of sample is made of bulk milkweed fibres compressed by hand to reach different bulk densities ρ_b ranging from 5.07 kg/m^3 to 43.13 kg/m^3. This type of sample is transversely isotropic since the orientation of the fibres is random in the transverse directions e_x and e_y, see Figure 2. For this first type of sample, its diameter and thickness are fixed to 44.44 mm and 25.4 mm, respectively. To increase the density, a given mass of bulk fibres are added in the fixed volume. For impedance tube tests, the volume is formed by the wall of the tube, the rigid piston backing, and a front grid as shown in Figure 2 (middle row). For static airflow resistivity tests, the thickness is fixed by a top grid and a rear grid. These grids are similar to the one used for the impedance tube.

The second type of sample is a nonwoven made of 70% in mass of milkweed and 30% in mass of bicomponent fibre (PP and PE). The averaged radius of the bicomponent fibre is 7.35 μm and its density $\rho_{s2} = 960$ kg/m^3. The fibres are mechanically mixed and carded into webs. Those webs are stacked and thermobonded to form a nonwoven with desired thickness and bulk density, which are respectively 25.4 mm and 17.13 kg/m^3. The samples thus formed

are relatively transversely isotropic. Unlike samples of the first type, those samples are self- supporting. This will facilitate porosity measurement tests and impedance tube tests in both directions. Figure 2 (bottom row) shows images of this second type of sample.

For the produced samples, the total open porosity (including the hollow part of the fibres) can be calculated from

$$\phi_t = 1 - \rho_b \left(\frac{p_1}{\rho_{s1}} + \frac{p_2}{\rho_{s2}} \right). \tag{14}$$

The term in parenthesis is the inverse of the equivalent density of the solid phase of the mixture composed of two types of fibres (here milkweed and bicomponent fibres). p_1 and p_2 are the mass proportions of each fibre, and ρ_{s1} and ρ_{s2} are the densities of their solid part, as given above. Note that for samples of the first type (milkweed fibres only), $p_1 = 1$ and $p_2 = 0$, while for the second type (milkweed and bicomponent fibres), $p_1 = 0.7$ and $p_2 = 0.3$.

Since it is initially assumed that only the air between fibres impacts on the acoustic propagation (to be verify later on), the open porosity to take into account should be the inter-fibre porosity only (i.e., the kinematic porosity). It is analytically deduced from

$$\phi_m = 1 - \rho_b \left(\frac{p_1}{\rho_{s1}\left(1 - \phi_\mu\right)} + \frac{p_2}{\rho_{s2}} \right). \tag{15}$$

With the previous two equations and the numerical numbers given above, the total open porosity of the samples of the first type ranges from 0.9705 to 0.9965, while the mesoporosity ranges from 0.8767 to 0.9855. Similarly, for the second type, the total open porosity is 0.9864, while its mesoporosity is 0.9604. As one can note, if the hollowness of the fibre does not affect the acoustic propagation, using the total porosity in acoustic models could yield erroneous predictions. This is one issue we attempt to elucidate in the following.

3.2. Porosity measurement

Porosity is measured with two different methods. The first one is achieved with an Argon porosity meter based on the Pressure/Mass method [12]. This method is well adapted to measure the total open porosity ϕ_t and bulk density ρ_b of the hollow fibre structures. The second method uses the indirect ultrasonic reflection technique described by Fellah *et al.* [13]. Here, since porosity is deduced from ultrasonic measurements, it yields the kinematic porosity ϕ_B - i.e., the open porosity seen by the acoustic wave propagating in the material. All porosity measurements are made with the self-supporting thermobonded nonwoven sample.

3.3. Resistivity measurement

The static airflow resistivity is measured with a resistivity meter following ASTM C522-03 standard[14] at the flow speed of 0.5 mm/s. The bulk fibres are added and compacted by hand within a sample holder that keeps material at fixed diameter (44.44 mm) and thickness (25.4 mm). The diameter of the tested samples are smaller than the 100-mm diameter suggested by the ASTM standard. This is done with a view to measure the sound absorption on samples similar to those used for absorption tests in an impedance tube of 44.44 mm in diameter. For each bulk density tested, the final resistivity result is obtained by averaging the resistivity measured on 7 samples.

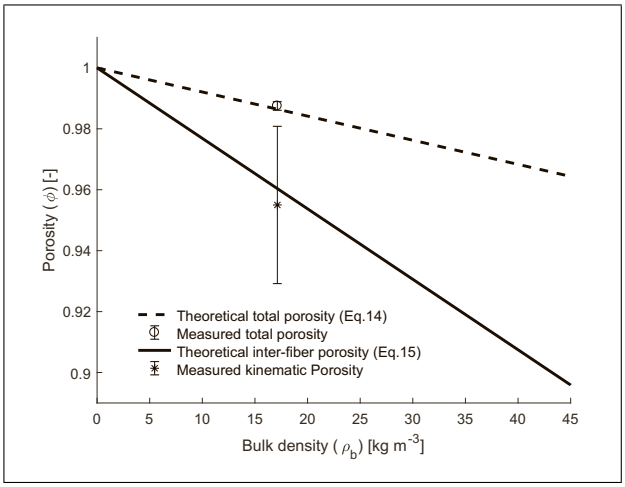

Figure 3. Theoretical and experimental open porosities of the thermobonded nonwoven as a function of the bulk density. Dashed line: theoretical total open porosity. Circle: experimental total open porosity by pressure/mass method. Solid line: theoretical inter-fibre porosity. Star: experimental kinematic porosity by ultrasound method.

3.4. Sound absorption measurement

Normal incidence sound absorption is measured between 250 and 4100 Hz with a 44.44-mm diameter impedance tube following standard ASTM E1050- 12[15]. For the first type of sample, as for the resistivity tests, the bulk fibres are added by hand into the tube, and then compacted between a grid and the tube's piston at the right density and thickness. A visual description of the setup is shown in Figure 2 (middle row). Note that the grid is nearly acoustically transparent (99.4% acoustically transparent, sound transmission loss less than 0.05 dB) and was not shown to affect the sound absorption of the test samples. For the second type of sample, 44.44-mm diameter specimens were cut from the fabricated non-woven material, in the normal z-direction, and in the transverse xy-direction. The specimens were then inserted in the tube and backed by the rigid piston of the tube. For each type of sample of the same bulk density, the final absorption curve is the average over 3 specimens.

4. Results

4.1. Open porosity

Figure 3 compares the measurements of the open porosity with the theoretical values of the total open porosity and

inter-fibre porosity (Equations (14) and (15), respectively) for the thermobonded nonwoven ($\rho_b = 17.13\,\mathrm{kg/m^3}$). First, one can note that the theoretical difference between total open porosity ϕ_t (dashed line) and mesoporosity ϕ_m (solid line) increases with the bulk density. Second, one can note that the total open porosities measured with the pressure/mass method (circles) are in line with the theoretical value at the tested density. Third, the porosity measured with the ultrasound method on five specimens is 0.955 ± 0.026 (uncertainty enlargement factor of 2). It is lower than the total open porosity and falls statistically on the theoretical inter-fibre porosity. Therefore, one can conclude that the inter-fibre porosity is the kinematic porosity, the one to use in acoustic porous models. This seems logical since the inner diameter of the hollow fibres is very small, and also because the fibres are highly diluted in the volume. As a consequence of the previous observations, and as expected, the studied hollow fibres can be considered as solid fibres with $\phi_\mu = 0$, and that the open porosity of the medium is only given by the inter-fibre porosity.

4.2. Resistivity

The results of the resistivity measurements on the bulk fibres compacted by hand are shown in Figure 4. These results are compared to those obtained from the corresponding micro-macro relationship along direction e_z (Equation 1). This relationship is fed with the mesoporosity ($\phi_m \to \phi$) and for the lower and upper limits of the fibre angular orientation ($\Omega_{zz} = 0$ and $\Omega_{zz} = 1$). It can be seen that experimental data (circles) are close to the $\Omega_{zz} = 0$ limit of the micro-macro model, especially at higher bulk densities. It can be explained by the fact that the fibre structure becomes more planar as compaction increases. At low bulk densities, we believe that the measured resistivities are underestimated due to the difficulty of obtaining a homogeneous distribution of the fibres by our by-hand process. Consequently, some areas on the samples are more permeable and create leaks. This has the effect of reducing the airflow resistivity. Consequently, we can hypothesize that the resistivity of our samples, as well as the other parameters, can be modelled as a 2d-structure with $\Omega_{zz} = 0$ as shown in Figure 1.

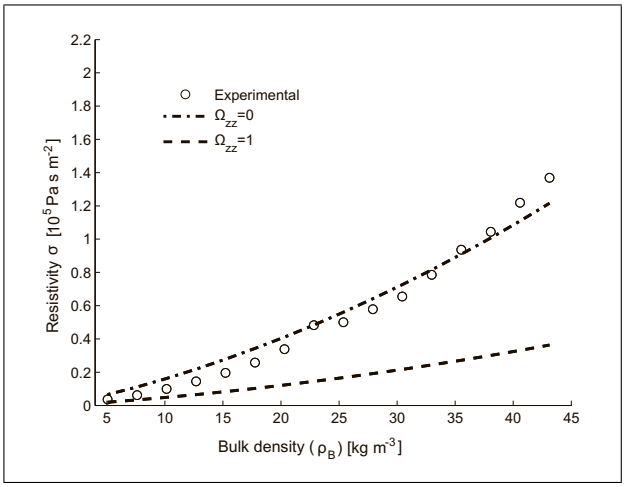

Figure 4. Resistivity of milkweed fibres compacted by hand in function of the bulk density and fibre orientation. Dashed line: $\Omega_{zz} = 1$. Dash-dot line: $\Omega_{zz} = 0$. Circles: experimental data.

4.3. Sound absorption

4.3.1. Effects of the hollow part of the fibres

In this subsection, only the hand-made and compacted milkweed fibre structures are used. Although 16 different bulk densities are tested and discussed, only the normal incidence sound absorption coefficients of three densities are presented in Figure 5 for illustrating the trends. The measured normal incidence sound absorption coefficients are compared to predictions using the Johnson-Lafarge model. Here, the 6 parameters of the Johnson-Lafarge model are obtained from the micro-macro relationships (Equation 1 and Equations 3 to 6) for (1) the case where the fibres are considered to be solid (i.e., $\phi_\mu = 0$), and (2) for the case where the fibres are considered hollow. In both cases, the material parameters along direction e_z are deduced from Equations (1) to (6), and only the $\Omega_{zz} = 0$ fibre orientation is considered.

As noted in Figure 5, at low bulk densities, under 20 kg/m^3, the added effect of the hollow part of the fibres is barely noticeable on the sound absorption. However, as bulk density increases, inter-fibre mesoporosity decreases and airflow resistivity increases. In this case, the contribution of the hollow portion of the fibres becomes more apparent, but remains low in the density range tested.

It is worth mentioning that the local peaks and dips in the experimental absorption curves are due to the elastic behaviour of the fibrous structures. The dips are due to the quarter wavelength frame resonance [16], while the peaks are due to fibre resonances [17]. The latter resonnances can not be reproduced by the used equivalent fluid model which assumes a rigid (motionless) structure.

In general, for the densities studied, results shown in Figure 6 indicate that the hollow part of the milkweed fibres has very little effect on the normal incidence sound absorption. Accordingly, as observed earlier in section 4.1 from porosity measurements, the milkweed fibre may also be considered as a solid fibre from a sound absorption perspective.

4.3.2. Effects of the fibre orientation

The first purpose of this subsection is to investigate the effects of the fibre orientation on the normal incidence sound absorption coefficient. The second purpose is to verify if the sound absorption coefficient of the studied milkweed fibre structures can be properly predicted by the one-parameter (resisitivity) model of Miki [18]. Here, the two types of fabrication are tested: (1) the hand-made and compacted bulk fibre structures, and (2) the thermobonded nonwoven.

For both the Johnson-Lafarge and Miki models, the model parameters are calculated from the micro-macro relationships of Equations (1) to (6). Note that for the Miki

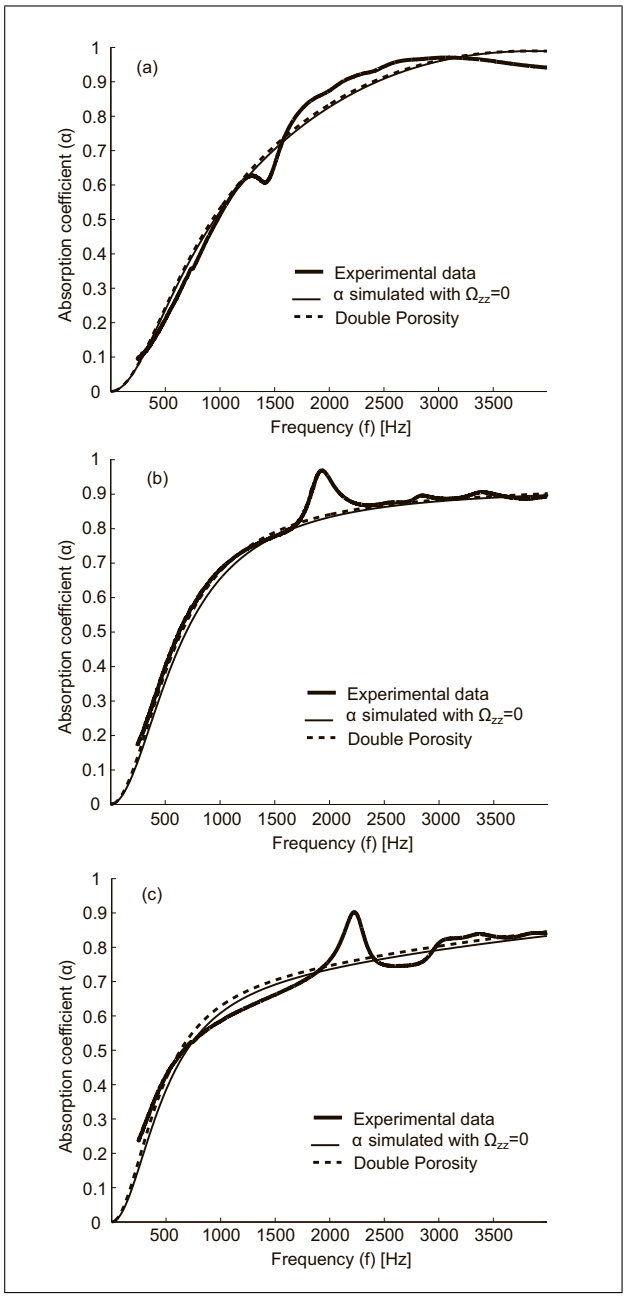

Figure 5. Effects of the hollowness of the milkweed fibres on the sound absorption of the bulk fibres compacted by hand for three bulk densities: a) 12.69 kg/m^3, b) 30.44 kg/m^3, and c) 40.59 kg/m^3. Thick line: experimental data. Thin line: micro-macro model with solid fibres and $\Omega_{zz} = 0$. Dashed line: micro-macro model for hollow fibres and $\Omega_{zz} = 0$.

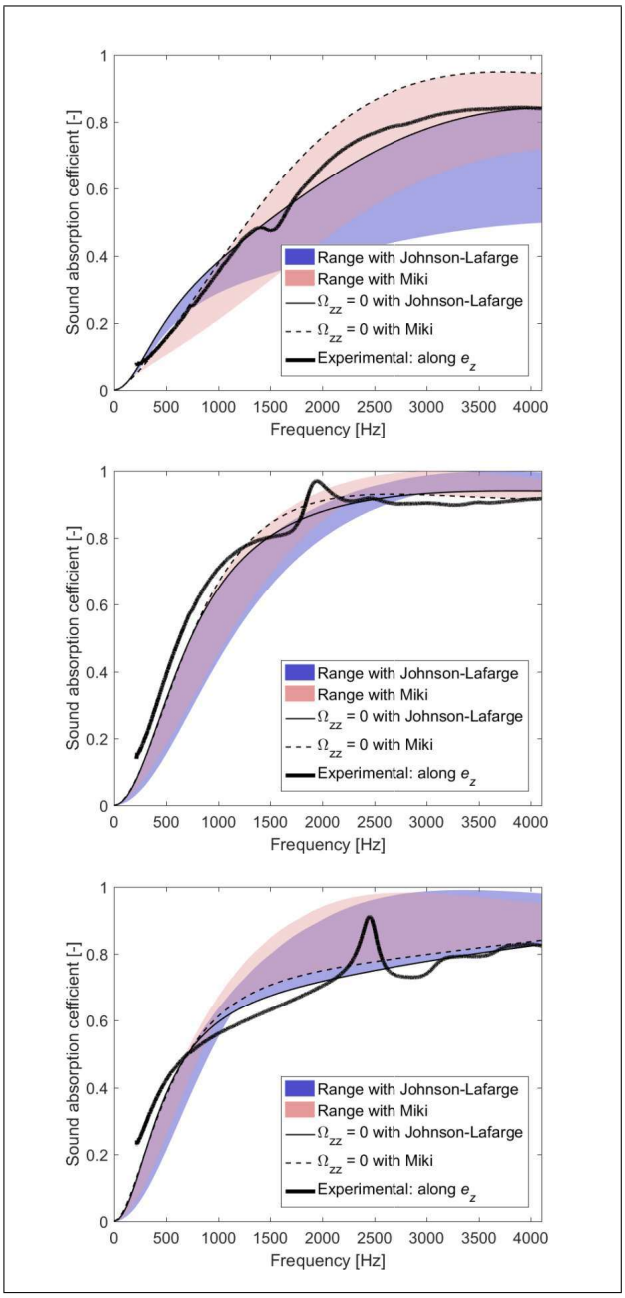

Figure 6. Effects of the fibre orientation on the sound absorption of the bulk milkweed fibres compacted by hand for three bulk densities: a) 7.61 kg/m^3, b) 25.37 kg/m^3, and c) 43.13 kg/m^3. Blue zone: range of sound absorption predicted by Johnson-Lafarge model for Ω_{zz} from 0 to 1. Pink zone: range of sound absorption predicted by Miki model for Ω_{zz} from 0 to 1. Thick line: experimental data. Solid line: Johnson-Lafarge model with $\Omega_{zz} = 0$. Dashed line: Miki model with predicted resistivity at $\Omega_{zz} = 0$.

model, only the calculated resistivity is needed. Based on the previous conclusion, the milkweed fibre is considered as solid ($\phi_\mu = 0$). For the hand-made and compacted bulk fibre structures, the material parameters (Equations 1 to 6) along direction e_z are used. For the thermobonded non-woven specimens, depending on the face exposed to the acoustical excitation in the tube (see Figure 2), material parameters along e_z or e_{xy} are used.

Figure 6 presents the normal incidence sound absorption of the hand-made compacted bulk milkweed fibres. Again, only the results for three densities are presented for the sake of conciseness and clarity. For the studied materials, one can observe that the fibre orientation may have a great impact on the sound absorption, and that a value of $\Omega_{zz} = 0$ (i.e., layered fibrous medium as in Figure 1) is the one which represents the best the tested material. This confirms the hypothesis that we issued at the very end of

Table I. Values of the transport parameters for normal and transverse directions.

	Normal	Transverse
σ (Pa s m^{-2})	47174	39053
α_∞	1.059	1.033
$\Lambda(\mu m)$	89	115

section 4.2, this is also consistent with the fabrication of the bulk fibre samples discussed in section 3.1.

Figure 6 also compares the six-parameter Johnson-Lafarge model to the one-parameter (resistivity) Miki model. One can note that both models yield comparable predictions; mainly at densities higher than 15 kg/m^3. For lower densities, it seems that the resistivity found by Equation (10) with $\Omega_{zz} = 0$ makes Miki's prediction overestimated. As discussed in section 4.2 and shown in Figure 4, at lower compaction levels (between 5 and 15 kg/m^3), the bulk fibre samples are less homogeneous and $\Omega_{zz} > 0$. As shown by the Ω_{zz} variation range with the Miki model on Figure 6a, a higher Ω_{zz} value will make Miki's prediction close to the measurement.

For the 17.13-kg/m^3 thermobonded nonwoven specimens described in section 3.1, the comparisons are presented in Figure 7a for the case along normal direction e_z, and 7b for the case along transverse direction e_{xy}. First, it can be noted that both rigid frame models, fed with the macroscopic parameters obtained by the micro-macro relationships with $\Omega_{zz} = 0$, give good predictions of the measurements, in spite of the frame resonances. More particularly, it seems the Miki model works particularly well in both directions. Second, the effects of the fibre orientations seems negligible for the transverse configuration since the transverse resistivity is not affected by the fibre orientation, see Equation (2). Only the viscous length and tortuosity are affected by the fibre orientation in this case. Transport parameters values are shown in Table I to show how properties vary from the normal to the transverse directions.

5. Conclusion

In this study, the validity of the micro-macro relationships by Luu *et al.* [4] for solid fibre assemblies is confirmed for the case of milkweed seed hair, a natural hollow fibre. Despite the obvious advantage of the fibre hollowness on bulk density, hollowness can be neglected without inducing major error on acoustical properties. Therefore, milkweed seed hair can be considered as a solid fibre from an acoustic perspective.

Also, the comparison with the experimental results shows that the one-parameter model of Miki as well as the 6 parameter model of Johnson–Lafarge, fed by the micro-macro relationships of Luu *et al.*, can be used to estimate the sound absorption of the studied fibrous structures.

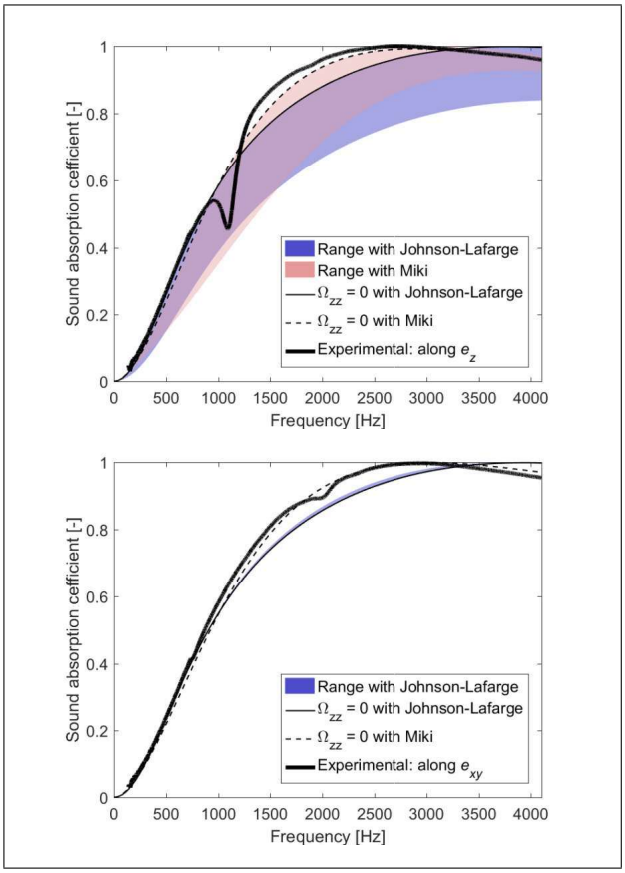

Figure 7. Comparison of a) normal absorption and b) transverse absorption for a nonwoven with a density of 17.13 kg/m^3. Blue zone: range of sound absorption predicted with Johnson-Lafarge model for Ω_{zz} from 0 to 1. Pink zone: range of sound absorption predicted with Miki model for Ω_{zz} from 0 to 1. Thick line: experimental data. Solid line: Johnson-Lafarge model for single porosity with $\Omega_{zz} = 0$. Dashed line: Miki model with predicted resistivity at $\Omega_{zz} = 0$.

Acknowledgement

This work was partly supported by grants-in-aid from Natural Sciences and Engineering Research Council of Canada (NSERC) and Fonds de recherche Nature et technologies du Québec (FRQNT). It was also made possible thanks to the participation of Mecanum Inc. who provided access to its characterization laboratory by the way of a master grade internship. The fibre used in this research was provided by Protec-Style.

References

[1] F. Asdrubali, S. Schiavoni, K. Horoshenkov: A review of sustainable materials for acoustic applications. Build. Acoust. **19** (2012) 283–312.

[2] X. Liu, X. Yan, H. Zhang: Sound absorption model of kapok-based fiber nonwoven fabrics. Text. Res. J. **85** (2015) 969–979.

[3] X. Liu, X. Yan, L. Li, H. Zhang: Sound-Absorption Properties of Kapok Fiber Nonwoven Fabrics at Low Frequency. J. Nat. Fibers **12** (2015) 311–322.

[4] H. T. Luu, C. Perrot, R. Panneton: Influence of porosity, fiber radius and fiber orientation on the transport and acoustic properties of random fiber structures. Acta Acustica united with Ac. **103** (2017) 1050–1063.

[5] H.T. Luu, C. Perrot, V. Monchiet, R. Panneton: Three-dimensional reconstruction of a random fibrous medium: Geometry, transport, and sound absorbing properties. J. Acoust. Soc. Am. **141** (2017) 4768–4780.

[6] H. T. Luu, R. Panneton, C. Perrot: Effective fiber diameter for modeling the acoustic properties of polydisperse fiber networks. J. Acoust. Soc. Am. **141** (2017) EL96–EL101.

[7] D. L. Johnson, J. Koplik, R. Dashen: Theory of dynamic permeability and tortuosity in fluid-saturated porous media. J. Fluids. Mech. **176** (1987) 379–402.

[8] D. Lafarge, P. Lemarinier, J. F. Allard, V. Tarnow: Dynamic compressibility of air in porous structures at audible frequencies. J. Acoust. Soc. Am. **102** (1997) 1995–2006.

[9] X. Olny, C. Boutin: Acoustic wave propagation in double porosity media. J. Acoust. Soc. Am. **11** (2003) 73–89.

[10] T. Karthik, R. Murugan, Milkweed - A potential Sustainable Natural Fiber Crop. In: Sustain. Fibres Fash. Ind., S. S. Muthu, M. A. Gardetti (eds.) Springer, 2016, p. 145.

[11] T. Dupont, P. Leclaire, R. Panneton: Acoustic methods for measuring the porosities of porous materials incorporating dead-end pores. J. Acoust. Soc. Am. **133** (2013) 2136–2145.

[12] Y. Salissou, R. Panneton: Pressure/mass method to measure open porosity of porous solids. J. Appl. Phys. **101** (2007) 124913.

[13] Z. E. A. Fellah, S. Berger, W. Lauriks, C. Depollier, C. Aristégui, J. Y. Chapelon: Measuring the porosity and the tortuosity of porous materials via reflected waves at oblique incidence. J. Acoust. Soc. Am. **113** (2003) 2424–2433.

[14] ASTM C522-03(2016) Standard Test Method for Airflow Resistance of Acoustical Materials, ASTM International, West Conshohocken, PA, 2016, https://doi.org/10.1520/C0522-03R16.

[15] ASTM E1050-12 Standard Test Method for Impedance and Absorption of Acoustical Materials Using a Tube, Two Microphones and a Digital Frequency Analysis System, ASTM International, West Conshohocken, PA, 2012, https://doi.org/10.1520/E1050-12.

[16] J.-F. Allard, N. Atalla: Propagation of Sound in Porous Media: Modelling Sound Absorbing Materials, 2nd ed. John Wiley and Sons, New York, 2009, page 130.

[17] M. D. Dahl, E. J. Rice, D. E. Groesbeck: Effects of fiber motion on the acoustical behaviour of an anisotropic, flexible fibrous material. J. Acoust. Soc. Amer. **87** (1990) 54–66.

[18] Y. Miki: Acoustical properties of porous materials. Modifications of Delany-Bazley models. J. Acoust. Soc. Japan **11** (1990) 19–24.